Received November 1, 2021, accepted November 14, 2021, date of publication November 23, 2021,
date of current version December 3, 2021.

Digital Object Identifier 10.1109/ACCESS.2021.3130370

Modified Q–f Droop Curve Method for Islanding Detection With Zero Non-Detection Zone

KIANOUSH NARAGHIPOUR[1], IBRAHIM ABDELSALAM[2], (Senior Member, IEEE), KHALED H. AHMED[1], (Senior Member, IEEE), AND CAMPBELL D. BOOTH[1], (Senior Member, IEEE)

[1]Department of Electronic and Electrical Engineering, University of Strathclyde, Glasgow G1 1XQ, U.K.
[2]Department of Electrical Engineering, Arab Academy for Science, Technology and Maritime Transport, Sheraton Campus, Cairo 11757, Egypt

Corresponding author: Kianoush Naraghipour (kianoush.naraghipour@strath.ac.uk)

This work was supported by the Engineering and Physical Science Research Council (EPSRC) under Grant EP/L015471/1.

ABSTRACT In this paper, a modified Q-f droop curve method for the inverter-based distributed generator is proposed. The proposed method has merits such as detecting islanding with zero non-detection zone, negligible effects on power quality, and simple implementation. A new parameter is embedded in the reactive power reference to accelerate the frequency deviation at the point of common coupling until the islanding is detected. Therefore, a passive under/over frequency relay will be simply sufficient to detect islanding within the permissible limit. The proposed method is modelled with a computer-aided design SIMULINK/MATLAB environment. The proposed method is analyzed for operation with unity and non-unity power factors. The performance is validated for various loading quality factors with a negligible change in detection time. In addition, it is confirmed that the proposed system is stable under unbalanced loading and switching conditions. The proper operation of the proposed islanding detection method under multi distributed generators connection is validated. The results of the hardware experimentations are presented to confirm the proposed method analysis and simulations.

INDEX TERMS Distributed generator (DG), non-detection zone (NDZ), point of common coupling (PCC), under/over frequency (UOF), under/over voltage (UOV).

I. INTRODUCTION

One of the serious concerns of electrical network utilities is unintentional islanding in the grid as it can cause a hazard for utility line-workers and damage distributed generator (DG) particularly during the DG reconnection [1]. In addition, for distributed generators in a microgrid, an unintentional islanding detection is important to transfer the operation safely and smoothly into islanded mode [2]. IEEE 1547 considers the islanding detection and its respective parameters, which include detection time, quality factor, and voltage/frequency thresholds. The islanding detection methods are classified into remote and local methods [3]. The latter can be further divided into passive and active methods. Remote methods are based on communication systems to monitor the network circuit breaker or recloser, when they are open during islanding. In [4], the islanding detection signal has been combined with a voltage unbalance of PCC voltage to help the local method for islanding detection. The main advantage of communication-based methods is that zero non-detection zone (NDZ) is achievable. However, the communication link adds complexity, cost, and reliability issues [5]. The passive methods include under/over voltage, under/over frequency, voltage phase jump detection or voltage vector shift, changes in voltage and current of total harmonic distortion, and rate of change of frequency [5]. When the power mismatch between the local load and DG is too small, the amount of frequency or voltage deviation will not be large enough to trigger the islanding detection method [6]–[8]. In [9]. a passive islanding detection method was introduced, which is based on a phasor measurement unit (PMU). It has a good performance for islanding detection, however, its detection time can be longer than active islanding detection methods. In [10], a passive islanding detection method was modelled based on components of the voltage signals. The islanding detection time is short with zero NDZ, however, it needs more performance investigation with different loading quality factors and multi DGs connection.

The associate editor coordinating the review of this manuscript and approving it for publication was Vitor Monteiro.

Signal processing methods have been developed to improve the operation of passive islanding detection methods [11]. However, their weakness under transient operation is the main challenge. In [12], a passive islanding detection method with logistic regression method, which is based on the machine learning technique has been introduced. It has a good performance, however, the system has not been tested for higher loading quality factors and multi DGs connection. In [13], an intelligent islanding detection method was presented, which is categorised under passive methods. It has an effective performance for islanding detection, although its operation under non-unity power factor of DG for different loading quality factors has not been considered.

In active methods, a small disturbance is injected into the point of common coupling (PCC) and then monitoring the DG electrical variables such as voltage and frequency to detect islanding. The most common active islanding detection methods with frequency deviation are active frequency drift [14], Sandia frequency shift [15], and slip-mode frequency shift [16]. The active methods have smaller NDZ, however, they can degrade the power quality at the PCC [17]. In [18], a method based on active frequency drift was proposed, which has been modified by the positive feedback, to improve the islanding detection performance. However, it does not show the effectiveness of the method for different loading quality factors.

Recently, active methods based on reactive power variation (RPV) have received noticeable consideration due to their high performance and simple implementation [19]–[26]. Nevertheless, the RPV methods still pose many challenges to attract noticeable research attention e.g. shortening the detection time and reducing the effect on the power quality.

In [19], a Q–f droop curve was embedded in the control algorithm to deviate the frequency during islanding. A conservative loading quality factor value has been set at 7.4 in the reactive power reference equation. The results confirm that higher loading quality factors will lead to an increase in the detection time or even to fail the islanding detection. The setting of the loading quality factor is based on trial and error, which makes it difficult the set this method for different rated active power of DGs and/or different grid frequencies and respective UOF thresholds.

In [20] and [21], the proposed islanding detection methods were based on an intermittent bilateral and unilateral variation of reactive power reference, respectively. In these two methods, DG reactive power was changed periodically. The main advantage is that zero NDZ is achievable. However, synchronization of periodic RPV based methods for multi DG connection is difficult. In [20], the loading quality factor was set at 2.5, whereas based on IEEE Std. 929-2000 [33], it can be 2.5 or less. Therefore, effective performance for a wide range of loading quality factors has not been presented.

The presented islanding detection method in [22], was based on the relationship between the reactive power disturbances and the frequency variation during islanding. The reactive power disturbances were configured periodically at two sets with different amplitude and duration time. Its advantage is a good islanding detection for the DG operation either at unity power factor or supplying reactive power for its local load with zero NDZ. As two sets of disturbances were periodic, its disadvantage is similar with [20] and [21]. In [22], the loading quality factor was set at 2.5 for all test cases during the unity power factor of DG performance. The performance has not been shown under different loading quality factors and their impact on detection time. In [23], an intelligent controller method was introduced for islanding detection. The controller deviates the frequency by adding a disturbance signal in the d-axis current when islanding happens. It has a rapid islanding detection speed, although, it still suffers from NDZ. Also, in [23] the islanding detection has been tested with only one value of loading quality factor.

In [24], the presented islanding detection method was based on the inverter's q-axis current controller, which was modelled with a continuous periodic reference current of a small value. The PCC frequency is deviated with respect to the variation of reference current during islanding. Also, an average absolute frequency deviation value was proposed during an islanding condition. The advantage of this method is its ability to detect islanding, when active and reactive powers mismatch are zero. Although, its performance under multi DG connection has not been investigated. The islanding detection algorithm in [25] was presented to eliminate NDZ during a reactive power mismatch by deviating the frequency beyond the thresholds. This method has zero NDZ, however it may degrade the power quality. In [25], the loading quality factor is set at 1, which is less than 2.5 as the higher value for the determined loading quality factor by [33]. In [26], a hybrid method was presented based on reactive power variation and four passive criteria. Despite rapid islanding detection time with zero NDZ, this method has complexity due to using various criteria. Also, in [26], the parameters of reactive power reference were set based on $Q_f = 2.5$. It means the performance of reactive power reference is different and the islanding detection time might be longer. The islanding detection method in [27] was proposed to eliminate the current static error in the frequency shift islanding detection method. It has a fast detection time with a very good performance. It needs more investigation under multi DGs connection mode. In [28], a hybrid method including voltage unbalance/Total Harmonic Distortion and bilateral reactive power variation was introduced. It has a fast detection time; however, its performance under multi DGs connection has not been considered.

It can be concluded that research efforts in literature have focused on operation with one value for the loading quality factor, whereas the loading quality factor can be changed in a wide range of load parameters. On the other hand, the setting of parameters in some methods is based on trial and error. Therefore, with changing the system frequency or UOF thresholds, a revised setting is required, which is time consuming.

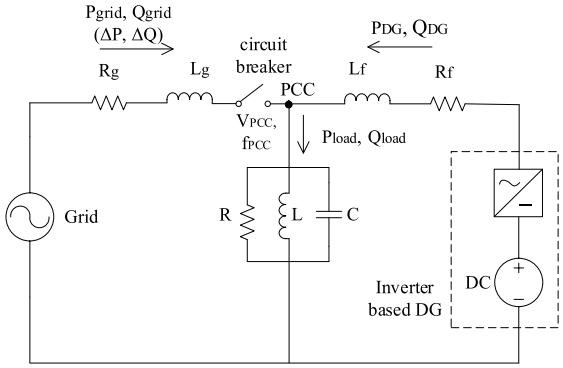

FIGURE 1. System study for islanding detection.

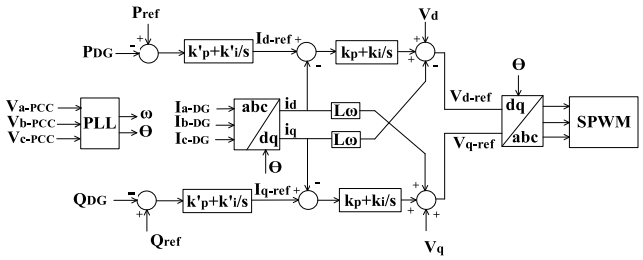

FIGURE 2. DG interface control system with inner and outer control loops.

In this paper, a modified Q–f droop curve method is proposed which its reactive power reference is set based on the converter rated power output, loading quality factor, load resonant frequency, and UOF thresholds. The proposed method is examined under different loading conditions and various loading quality factors. Its ability for islanding detection with zero NDZ and rapid detection time is presented. Also, its implementation for multi DG connection is demonstrated.

The contributions of the paper are as follows: 1) proposed a modified islanding detection method. 2) the experimental validation of the proposed islanding detection method for both static and dynamic loads.

The rest of this paper is organized as follows. Section II presents the islanding basic system modelling. Section III provides the proposed islanding detection method. Section IV presents performance and simulation results of the proposed method. Section V demonstrates the experimentally validation of the proposed islanding detection method, which is tested under different load conditions.

II. ISLANDING BASIC SYSTEM MODELLING

The system under investigation is illustrated in Figure 1. It consists of a three-phase grid, a parallel three-phase RLC load and an inverter-based DG, which is modelled as a constant DC source behind a three-phase inverter.

The DG interface control structure comprises two controllers as shown in Figure 2. The first control loop is an inner current controller to regulate the current while the second control loop is an outer power controller to regulate the active/reactive powers. The instantaneous active and reactive powers can be presented in terms of the dq axis components [29], as (1) and (2).

$$P_{DG} = \frac{3}{2} v_d i_d \tag{1}$$

$$Q_{DG} = \frac{3}{2} v_d i_q \tag{2}$$

The active and reactive powers for the RLC load, when the grid is connected to PCC can be calculated as in (3) and (4).

$$\mathrm{P_{load}} = \frac{\mathrm{V_{PCC}^2}}{\mathrm{R}} \tag{3}$$

$$Q_{load} = V_{PCC}^2 \left(\frac{1}{2\pi f_{PCC} L} - 2\pi f_{PCC} C \right) \tag{4}$$

Also, active and reactive powers of the load can be expressed based on active/reactive powers of the grid and DG as in (5) and (6):

$$P_{load} = \Delta P + P_{DG} \tag{5}$$

$$Q_{load} = \Delta Q + Q_{DG} \tag{6}$$

where, ΔP and ΔQ are the power mismatch between DG and load, which are provided by the grid, as shown in Figure 1. In grid-connected operation, the PCC frequency is determined by the grid. However, after islanding, the PCC frequency is stabilized at the resonant frequency when the DG is running at the unity power factor. In that case, the reactive power of the load is moving towards zero, thus:

$$Q_{DG} = Q_{load} = V_{PCC}^2 \left(\frac{1}{2\pi f_{PCC} L} - 2\pi f_{PCC} C \right) = 0 \tag{7}$$

$$f_{PCC} = f_{res} = \frac{1}{2\pi\sqrt{LC}} \tag{8}$$

If the resonant frequency is within the under/over frequency (UOF) thresholds, then it will not be detected by the UOF relay. Another important parameter that affects the NDZ is the loading quality factor ($\mathrm{Q_f}$). It is defined as the ratio of the maximum stored energy to the dissipated energy.

$$Q_f = \left(\frac{1}{P_{load}} \right) \sqrt{|Q_{L-load}|\,|Q_{C-load}|} \tag{9}$$

Also, the quality factor can be expressed as in (10).

$$Q_f = R\sqrt{C/L} \tag{10}$$

According to IEEE Std. 929-2000 [33] requirement, $\mathrm{Q_f}$ is set at 2.5 for an islanding detection test. However, the islanding detection method must provide an effective performance for all amounts of $\mathrm{Q_f} < 2.5$ as well. The relationship between loading quality factor, reactive power mismatch and frequency thresholds can be obtained as in (11) [31]:

$$P_{DG} Q_f \left(1 - \left(\frac{f_{grid}}{f_{min}} \right)^2 \right) \le \Delta Q \le P_{DG} Q_f \left(1 - \left(\frac{f_{grid}}{f_{max}} \right)^2 \right) \tag{11}$$

where, $\mathrm{f_{grid}}$ is the grid frequency, $\mathrm{f_{min}}$ and $\mathrm{f_{max}}$ are the upper and lower frequency thresholds of UOF relay. As shown

in (11), $P_{DG}Q_f$ for DG rated power and loading quality factor can be equal for DG with different rated powers and loading quality factors. For example, the multiplication of a DG with $P_{DG} = 100$ kW and $Q_f = 2.5$ is same as a DG with $P_{DG} = 200$ kW and $Q_f = 1.25$. Therefore, inequality in (11) for a DG with maximum quality factor ($Q_f = 2.5$) is not able to guarantee proper islanding detection for other DGs with different rated powers. For this reason, any islanding detection method must be examined for various loading quality factors, lower and higher than 2.5, to validate its effectiveness with different DG rated powers.

III. PROPOSED MODIFIED Q-F DROOP CURVE METHOD FOR ISLANDING DETECTION

As mentioned in the introduction, RPV is an attractive islanding detection method, in which the reactive power of DG varies after the grid disconnection and it drifts the PCC frequency beyond the UOF relay threshold. In [19], the load reactive power has been calculated as in (12).

$$Q_{load} = -2P_{DG}\frac{Q_f}{f_{res}}\left(f_{PCC} - f_{res}\right) \tag{12}$$

As expressed in (12), the load Q-f equation has been calculated as a function of the load's resonant frequency. Also, the DG reactive power reference has been defined by:

$$Q_{ref} = k_1 f_{PCC} + k_2 \tag{13}$$

where, the values of k_1 and k_2 have been considered for constant P_{DG} and Q_f. It means that for different P_{DG} rated values, different Q_f values have to be used, which is difficult and relies on a trial and error approach. Therefore, it is essential to find an optimized method for calculating k_1 and k_2, which depends on grid and load parameters rather than trial and error. Also, in [19], f_{res} does not have any role for the calculation of k_2. On the other word, for any UOF thresholds or any grid frequency, k_2 is not changed and it is a constant value. It is another challenge, which makes it difficult to operate in other system frequencies.

In [25], another reactive power reference equation has been proposed to enhance the performance as in (14).

$$Q_{ref} = -k_1\left(f_{PCC} - k_2\right) + Q_{load} \tag{14}$$

where, k_1 is a positive constant value and k_2 is set below or above the frequency threshold depending on PCC phase voltage during islanding. However, the value of k_1 has been specified for a constant P_{DG} and Q_f by trial and error. Therefore, it is not suitable for different loading quality factors. In both methods above, it is difficult to find optimum values for k_1 and k_2 to detect islanding for different DG rated powers. Also, in [25] with a high value for k_1, which is equal to 1000, the power quality might be degraded.

If there is a reactive power mismatch between DG output and local loads, when islanding happens, the reactive power mismatch makes a change in the frequency of the PCC voltage. Therefore, after islanding, the frequency of PCC voltage is shifted to a new value, f'_{PCC}. In that case, the inductive

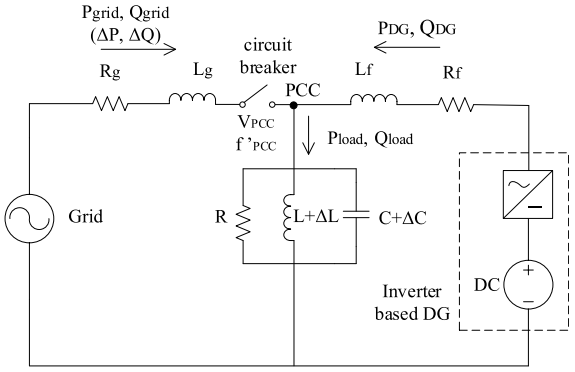

FIGURE 3. Islanding circuit after grid disconnection with reactive power mismatch.

parameters of the load can be represented by $L + \Delta L$ and $C + \Delta C$ [30] as illustrated in Figure 3.

Accordingly, the resonant frequency is modified as [30]:

$$f'_{PCC} = f_{res-modified} = \frac{1}{2\pi\sqrt{(L+\Delta L)(C+\Delta C)}} \tag{15}$$

The ratio of resonant frequency without and with power mismatch can be expressed:

$$\frac{f_{res}}{f_{res-modified}} = \frac{\sqrt{(L+\Delta L)(C+\Delta C)}}{\sqrt{LC}} \tag{16}$$

For simplicity, ($\Delta L \Delta C \approx 0$), then (16) can be:

$$\left(\frac{f_{res}}{f_{res-modified}}\right)^2 = 1 + \frac{\Delta L}{L} + \frac{\Delta C}{C} \tag{17}$$

On the other hand, equation (10) can be expressed as:

$$Q_f^2 = \frac{R^2 C}{L} \tag{18}$$

Also (8) can be expressed as:

$$C = \frac{1}{L\omega_{res}^2} \tag{19}$$

With substitution (19) in (18):

$$Q_f = \frac{R}{X_L} \tag{20}$$

Similarly, it can be obtained:

$$Q_f = \frac{R}{X_C} \tag{21}$$

Thus:

$$P_{DG}Q_f = Q_L = Q_C \tag{22}$$

The effect of resonant frequency on reactive power mismatch can be represented as:

$$\Delta Q = V_{PCC}^2\left(\frac{1}{2\pi f L\left(1+\frac{\Delta L}{L}\right)} - 2\pi f C\left(1+\frac{\Delta C}{C}\right)\right) \tag{23}$$

With substitution (22) in (23):

$$\Delta Q = \frac{P_{DG}Q_f}{\left(1+\frac{\Delta L}{L}\right)} - P_{DG}Q_f\left(1+\frac{\Delta C}{C}\right) \tag{24}$$

Then,

$$\frac{\Delta Q}{P_{DG}Q_f} = -\left(\frac{\Delta L}{L}+\frac{\Delta C}{C}\right) \tag{25}$$

For simplicity, $\left(1+\frac{\Delta L}{L}\approx 1\right)$, and with substitution (25) in (17):

$$\left(\frac{f_{res}}{f_{res-modified}}\right)^2 = 1 - \frac{\Delta Q}{P_{DG}Q_f} \tag{26}$$

Equation (26) can be rewritten as:

$$-P_{DG}Q_f\left(\frac{f_{res}}{f_{res-modified}}\right)^2 + P_{DG}Q_f = Q_{load} - Q_{DG} \tag{27}$$

The curve between the load reactive power and PCC frequency is approximately linear within the UOF thresholds. To formulate a linear relation between PCC frequency and DG reactive power reference, a new equation is proposed with the same parameters of equation (27) to deviate the PCC frequency after the grid disconnection as in (28).

$$Q_{ref} = a_1 f_{PCC} + a_2 \tag{28}$$

where, $a_1 = -P_{DG}Q_f\left(\frac{f_{res}}{f_{res-modified}}\right)^2$ and $a_2 = P_{DG}Q_f$

Also, equation (28) should be modified such that the DG reactive power reference is equal to the pre-set original reactive power reference during the grid connected mode as in (29):

$$Q_{ref} = a_1 f_{PCC} - a_1 f_{grid} + Q_{ref-original} \tag{29}$$

Using equation (29), the PCC frequency will be deviated outside the UOF thresholds after grid disconnection even if there is no active/reactive power mismatch between the load and DG. Therefore, zero non-detection zone is achievable (NDZ = 0) when islanding occurs. Also, the proposed reactive power reference equation is a function of the grid parameters, UOF thresholds, and loading quality factor. Thus, the proposed islanding detection method enables to detect islanding for any value of PCC frequency and no need for trial and error to choose Q_f. Since $f_{res-modified}$ can be set based on upper and lower limits of UOF relay, equation (29) is split into two equations. When the PCC frequency is below the grid frequency, $f_{res-modified}$ is set at the upper threshold of UOF relay, whereas for PCC frequency equal or above the grid frequency, it is set at the lower threshold of UOF relay. The DG reactive power reference at upper limit of UOF is called $Q_{ref-upper}$ and for the lower limit is $Q_{ref-lower}$. The proposed reactive power reference equation's slope is designed to provide a higher negative slope than the load curve. Therefore, after islanding, when the PCC frequency is below the grid frequency, the reactive power reference value (equation (29)) is more than the reactive power of the load.

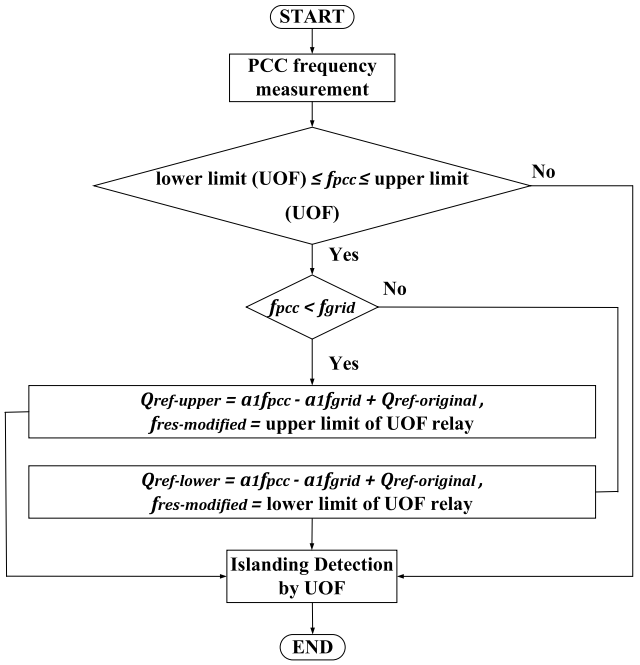

FIGURE 4. Flowchart of the proposed islanding detection method.

In that case, the PCC frequency moves toward the lower value in order to increase the load's reactive power. Then, the PCC frequency is drifted beyond the lower threshold and islanding can be detected smoothly. Correspondingly, when the PCC frequency is above the grid frequency, the reactive power reference value is less than the load reactive power. The PCC frequency has to move toward the upper value in order to draw the load's reactive power toward the reference reactive power. This result in that the PCC frequency is pushed to be more than the upper threshold and finally islanding is detected. Figure 4 is the flowchart of the proposed islanding detection method.

IV. PERFORMANCE AND SIMULATION RESULTS OF THE PROPOSED ISLANDING DETECTION METHOD

In this section, several cases are designed and modelled by using MATLAB/SIMULINK software to utilize the system shown in Figure 1. The grid and DG parameters are presented in Table 1. An island event is formed at t = 0.5 s, and the PCC frequency is 50 Hz before islanding. Equation (29) is used to calculate the upper and lower limits of the DG reactive power reference as in (30) and (31).

$$Q_{ref-upper} = -0.245 f_{PCC} + 12.25 + Q_{ref-original} \tag{30}$$

$$Q_{ref-lower} = -0.257 f_{PCC} + 12.85 + Q_{ref-original} \tag{31}$$

where, $Q_f = 2.5$ based on IEEE Std. 929-2000 [33], and $f_{res-modified}$ is set at the upper or lower limits of the frequency thresholds, which are 50.5 Hz and 49.3 Hz, respectively.

TABLE 1. Grid and DG parameters.

Grid Parameters	
Voltage	400 V
Frequency	50 Hz
Grid Resistance	0.02 Ω
Grid Inductance	0.3 mH
DG Inverter Controller Parameters	
Current Controller	kp=3, ki = 60
Power Controller	k'p = 5, k'i = 70
Rated Active Power	100 kW

TABLE 2. Load parameters.

$Q_{ref-original}$ (kVAr)	Q_f	f_{PCC} (Hz)	R (Ω)	L (mH)	C (μF)
0	1	49.8	1.6	5.1134	1997.4
	2.5			2.0454	4993.6
	3.5			1.4610	6991
	4.5			1.1363	8988.4
	1	50		5.0930	1989.4
	2.5			2.0372	4973.6
	3.5			1.4551	6963.0
	4.5			1.1318	8952.5
	1	50.2		5.0727	1981.5
	2.5			2.0291	4953.8
	3.5			1.4993	6935.3
	4.5			1.1273	8916.8
10	1	52.57		4.8440	1892.2
	2.5	51.01		1.9968	4875.1
	3.5	50.72		1.4345	6864.2
	4.5	50.56		1.1192	8853.3

A. PROPOSED ISLANDING DETECTION METHOD PERFORMANCE WITH DIFFERENT Q_{ref} AND Q_f

In order to comprehensively validate the proposed islanding detection method, several loading quality factors with different reactive power references are included. Also, the impact of PCC frequency variation after islanding, when it is close or equal to the grid frequency (the most difficult case) is tested. The simulated cases parameters at unity and non-unity power factors are shown in Table 2.

Figure 5 parts (a), (b), and (c) show the PCC frequency response, which is set at 49.8 Hz, 50 Hz, and 50.2 Hz respectively after islanding. Each case is tested at different four loading quality factors, while the DG operates with unity power factor. Figure 5 (a) illustrates that after the grid disconnection, the PCC frequency (f_{PCC} = 49.8 Hz) is less than the grid frequency, and the value of load reactive power is less than the proposed reactive power reference value. Thus, the frequency will decrease to increase the load's reactive power. The PCC frequency is finally drifting beyond the UOF threshold and islanding is detected. Figure 5 (b) presents the most difficult case, when the mismatch of active and reactive powers between load and DG is zero. For the loading quality factors equal 1, the PCC frequency is deviated beyond the upper threshold. In that case, after the grid disconnection, the proposed islanding detection method draws the PCC frequency to the upper threshold. With increasing the loading quality factor to 2.5, 3.5, and 4.5, the PCC frequency is

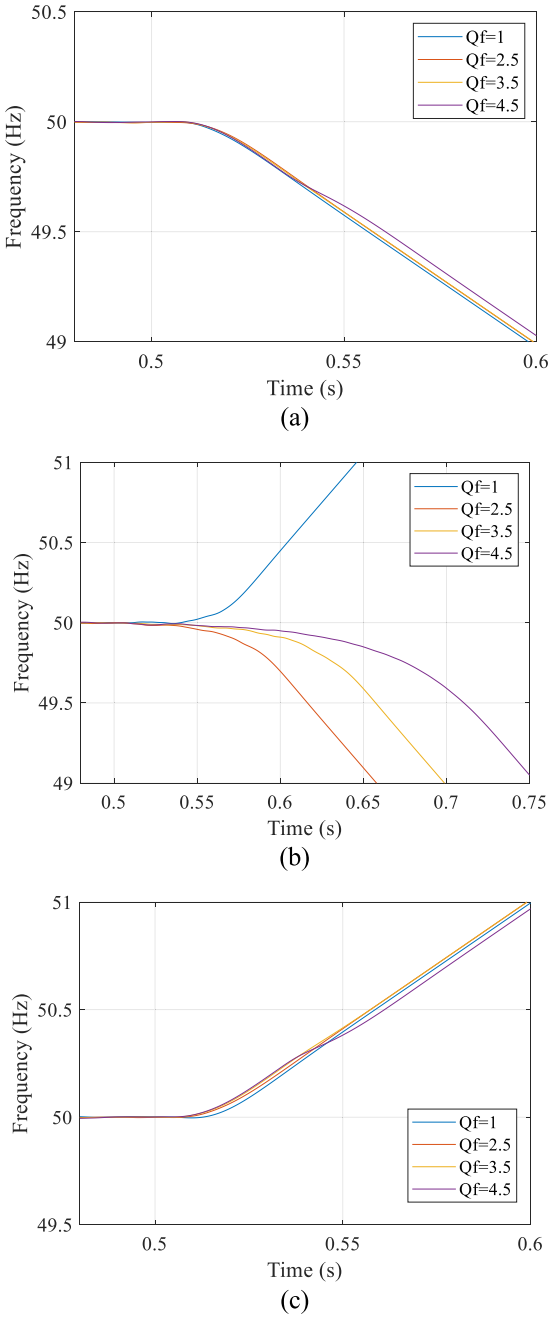

FIGURE 5. Frequency response with $Q_{ref-original}$ = 0 based on: (a) f_{PCC} = 49.8 Hz, (b) f_{PCC} = 50 Hz, and (c) f_{PCC} = 50.2 Hz.

deviated outside the lower frequency threshold. It is due to a small variation of PCC frequency toward the frequency below 50 Hz after the grid disconnection. For higher loading quality factors, the slope of load curve is increased, and approaches to the proposed method's slop curve. This increases the detection time. In Figure 5 (c), after the grid disconnection, the PCC frequency (f_{PCC} = 50.2 Hz) is more than the grid frequency and the value of load reactive power is more than the proposed reactive power reference value. As a result, the frequency will increase to decrease the load's

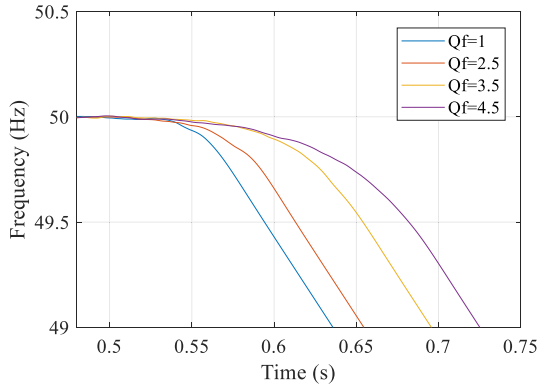

FIGURE 6. Frequency response with $Q_{ref-original} = 10$ kVAr.

TABLE 3. Detection time for different quality factors.

$Q_{ref-original}$ (kVAr)	Q_f	f_{PCC} (Hz)	Detection time (ms)			
			Proposed method	[19]	[25]	[26]
0	1	49.8	72	136	90	84
	2.5		75	Failed	94	80
	3.5		75		96	88
	4.5		77.5		101	90
	1	50	105	Failed	220	218
	2.5		133		228	208
	3.5		174		230	223
	4.5		229		246	230
	1	50.2	58.5	102	89	89
	2.5		59	Failed	92	75
	3.5		58.5		94	91
	4.5		62		102	95
10	1	52.57	110	Failed	156	149
	2.5	51.01	130		164	140
	3.5	50.72	170		175	172
	4.5	50.56	200		212	201

reactive power. The PCC frequency is finally drifting beyond the upper threshold and islanding is detected.

In order to test the proposed islanding detection method for other operating conditions, Figure 6 shows the frequency response when the DG operation is set with non-unity power factor ($Q_{ref-original} = 10$ kVAr). The load parameters are adjusted in such that the mismatch of active and reactive powers is almost zero as shown in Table 2. The PCC frequencies are selected to make around zero power mismatch condition after islanding for different loading quality factors. In that case, the PCC frequency drops below 50 Hz after the grid disconnection. Then, the proposed detection method forces the PCC frequency to move towards to the lower thresholds until islanding is detected.

Table 3 shows the detection time of the proposed islanding detection method compared to conventional methods [19], [25], and [26] for all cases in Figure 5 and Figure 6. It confirms that the detection time for all cases is faster than the required detection time (2 s) as recommended by IEEE Std. 929-2000 [33]. It shows also that the most rapid detection time is achieved when the PCC frequency is above the grid frequency. It is due to the less difference between the upper

TABLE 4. Unbalanced load parameters.

$Q_{ref-original}$ (kVAr)	Q_f	f_{PCC} (Hz)	R_a, R_b (Ω)	R_c (Ω)	L (mH)	C (μF)
0	1	50	1.39	1.6	5.0930	1989.4
	2.5				2.0372	4973.6
	3.5				1.4551	6963.0
	4.5				1.1318	8952.5
10	1	52.57			4.8440	1892.2
	2.5	51.01			1.9968	4875.1
	3.5	50.72			1.4345	6864.2
	4.5	50.56			1.1192	8853.3

frequency threshold (50.5 Hz) and the grid frequency (50 Hz) compared with the lower frequency threshold (49.3 Hz).

The islanding detection method in [19] fails to detect islanding when the PCC frequency is set at 49.8 Hz or 50.2 Hz for after islanding and loading quality factor is above 1. Also, it fails to detect islanding when the PCC frequency is set at 50 Hz with unity power factor or DG is working with non-unity power factor. It is due to a higher slope for the load curve, when the loading quality factor rises. In that case, the presented reactive power reference curve in [19] does not have a high slope enough compared with the load to deviate PCC frequency after the grid disconnection. It is getting worse for zero power mismatch conditions. Also, as previously mentioned, k_2 in reactive power reference [19] is not updated. In [25], the islanding detection method can detect the islanding. However, parameter k_1 has been set with a constant value without any relation to the loading quality factor or the rated active power of DG. Thus, for different loading quality factors, particularly for the higher of them, the detection time becomes longer.

The islanding detection method in [26] is able to detect islanding for all cases, but the detection time is longer than the proposed method. The parameters of reactive power reference [26] were set based on $Q_f = 2.5$. Therefore, with changing the loading quality factor, the setting of reactive power reference is changed. It makes the detection time longer. Therefore, the proposed Q-f droop curve method has better results, particularly for the higher loading quality factors compared with [19], [25], and [26].

B. PROPOSED ISLANDING DETECTION METHOD PERFORMANCE WITH UNBALANCED LOADS

To test the effect of unbalanced loading on the proposed islanding detection method, two phases of the load resistance are set at 115 kW ($R_a = R_b = 1.39\ \Omega$), whereas the third phase is set at 100 kW ($R_c = 1.6\ \Omega$). The unbalanced load is considered for both unity and non-unity power factors of DG operation. Also, it is simulated for the most difficult cases, when the PCC frequency after islanding is equal to 50 Hz as shown in Table 4.

Figure 7 shows that the proposed islanding detection method is able to detect islanding for both unity and non-unity power factor of DG operation with almost zero power mismatch. The PCC frequency measured after islanding with

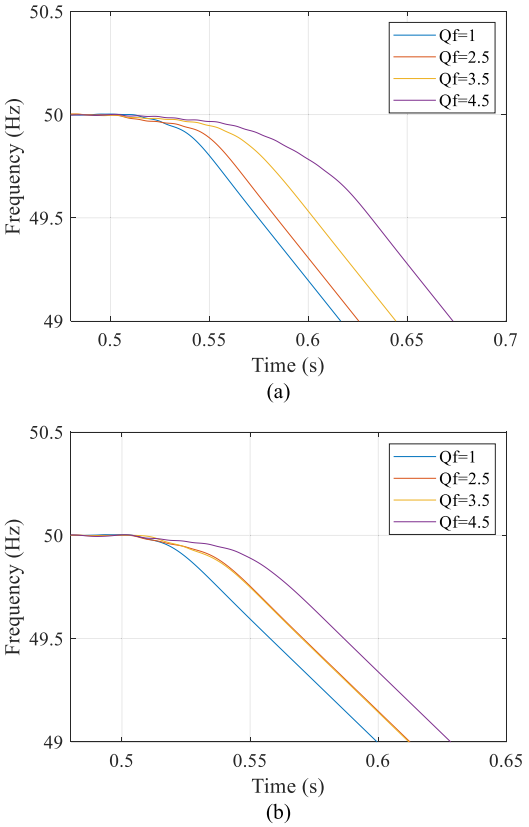

FIGURE 7. Frequency response for unbalanced load based on: (a) $Q_{ref-original} = 0$, and (b) $Q_{ref-original} = 10$ kVAr.

TABLE 5. Detection time for unbalanced load and different quality factors.

$Q_{ref-original}$ (kVAr)	Q_f	f_{PCC} (Hz)	Detection time (ms)			
			Proposed method	[19]	[25]	[26]
0	1	50	90	Failed	128	119
	2.5		100		142	104
	3.5		120		157	124
	4.5		149		174	150
10	1	52.57	74	88	112	91
	2.5	51.01	87	Failed	119	88
	3.5	50.72	87		130	92
	4.5	50.56	104		147	105

different values of loading quality factors is deviated toward below threshold of frequency. Also, it shows that with increasing the loading quality factors, the detection time becomes longer. It is due to the slope of the load curve rising for higher loading quality factors and approaching the proposed method's slop curve.

Table 5 shows the detection time of the proposed islanding detection method for unbalanced loading compared to conventional methods [19], [25] and [26]. It confirms that the detection time for all cases is faster than the required detection by IEEE Std. 929-2000 [33]. The islanding detection method in [19], when the PCC frequency is set at 50 Hz for unbalanced load during islanding, it is not able to detect islanding.

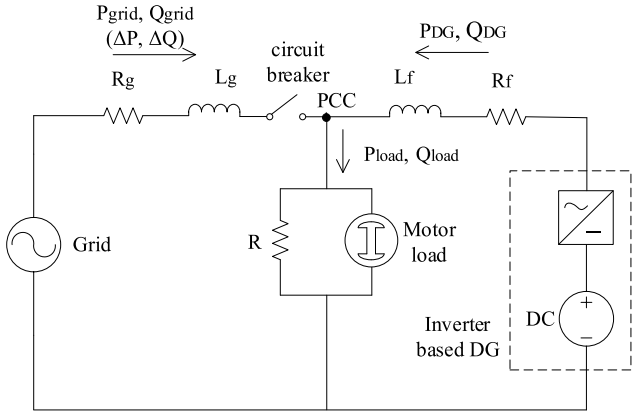

FIGURE 8. System study for islanding detection with motor load.

Also, for DG operation with non-unity power factor and unbalanced load conditions, it is only able to detect islanding, when loading quality factor is equal to 1.

Similar to the previous part, for zero power mismatch the presented method in [19] is not able to detect islanding. In the other word, after islanding, PCC frequency deviation is not big enough to be moved beyond the UOF threshold. It is due to improper setting of k_1 and k_2 for reactive power reference presented in [19]. In [25], the detection time is longer than the proposed method's detection time. As previously mentioned, the parameters in this method has been set for the loading quality factor equal 1. Thus, with increasing the loading quality factor, the detection time is increased. The islanding detection method in [26] is able to detect islanding for all cases, however its detection time is longer than the proposed method. Similar to the previous part, the proposed Q-f droop curve method has faster islanding detection without any fail, when a DG operates with both unity and non-unity power factor under the unbalanced load conditions. It is one of the main significant advantages of proposed method, particularly for the higher loading quality factors compared with [19], [25] and [26].

C. PROPOSED ISLANDING DETECTION METHOD PERFORMANCE WITH MOTOR LOAD

As realistic loads, such as motors constitute a substantial portion of the distribution system [32], the performance of the proposed islanding detection method is tested with an induction motor and resistance load as shown in Figure 8. The proposed method should be able to recognize between islanding detection and motor starting to avoid any unnecessary disconnection from the grid. Also, the proposed method must be capable to disconnect a dynamic load, such as a motor from the DG, when islanding occurs. The motor's torque is set at full load mode. The parameters of motor load chosen for the simulation are listed in Table 6.

Four cases are simulated. As shown in Figure 9 (a) in two cases, the load resistance power is set at 80 kW. In those two cases, the motor is in steady-state condition or the motor is

TABLE 6. Motor load parameters.

Type of Motor	Squirrel-Cage
Voltage	400 V
Frequency	50 Hz
Rated Power	15 kW (20 HP)
Speed (rpm)	1460

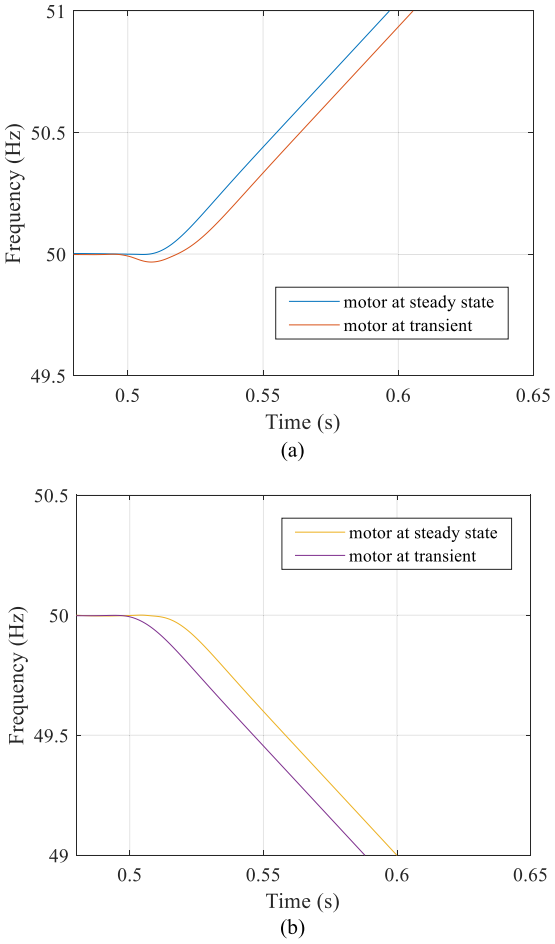

FIGURE 9. Frequency response: (a) load resistance power is set at 80 kW, and (b) load resistance power is set at 100 kW.

in transient (starting time is set at 0.49 s, which is 0.01 s before the grid disconnection). Also, Figure 9 (b) illustrates two cases, when the load resistance power is set at 100 kW and the motor conditions is as similar as the aforementioned conditions.

In Figure 9 (a), after the grid disconnection, when the resistance load and motor starting time are the same, PCC frequency is deviated above the upper threshold limit, when islanding occurs. It is due to the bigger value of DG rated active power (100 kW) compared to resistance and motor load active power. Therefore, the PCC voltage rises. When the motor starting time is very close to the grid disconnection time, the motor inrush current makes a voltage dip at the PCC voltage. Therefore, PCC frequency is deviated for a longer time. In Figure 9 (b), during the grid disconnection, when

TABLE 7. Detection time for motor load.

Resistance load (P_R)	Motor load (P_m)	Detection time (ms)	
		Motor & load resistance are connected to the grid at the same time	Motor starting at 0.49 s
80 kW	15 kW	55	65
100 kW		74	62

TABLE 8. Additional load parameters for load switching.

$P_{\text{additional–load}}$ (kW)	Power factor
100	1
50	1
80	0.8 lag
80	0.8 lead

the resistance load and motor starting time are the same, PCC frequency is deviated under the lower threshold limit. It is due to the smaller value of DG rated active power compared to resistance and motor load active power. Therefore, the PCC voltage drops. When the motor starting time is very close to the grid disconnection time, the motor inrush current is added to the PCC voltage reduction and it causes a shorter detection time. Table 7 shows the detection times for Figure 9.

D. PROPOSED ISLANDING DETECTION METHOD PERFORMANCE IN LOAD SWITCHING CONDITIONS

In this section, the proposed islanding detection method is tested under load switching conditions. The proposed method should be able to maintain PCC voltage and frequency within permissible limits during load switching and avoidance any inessential disconnection from the grid. An additional load is added to the circuit presented in Figure 1. The additional load is switched on at t = 0.5 s then turned off at t = 1 s. The response of PCC voltage and frequency are investigated for four loading cases as presented in Table 8. For all additional load cases, DG is operating with active rated power (100 kW) and loading quality factor equal to 2.5 during grid connection.

As presented in Figure 10, voltage and frequency are deviated, when the additional load is switched on and off within the UOV/UOF thresholds, whereas before and after switching the voltage and frequency operate at their rated values. Therefore, the proposed islanding method during load switching does not impact the power system performance during normal conditions.

E. PROPOSED ISLANDING DETECTION METHOD PERFORMANCE IN MULTIPLE DGs CONNECTION

The proposed islanding detection method is further tested for multiple DGs connection. The proposed method should

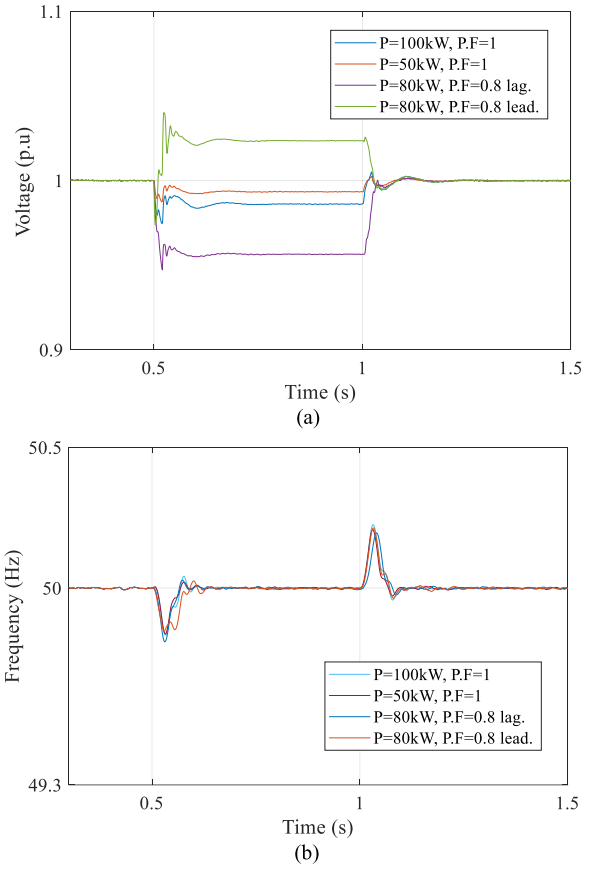

FIGURE 10. Load switching performance: (a) PCC voltage, and (b) PCC frequency.

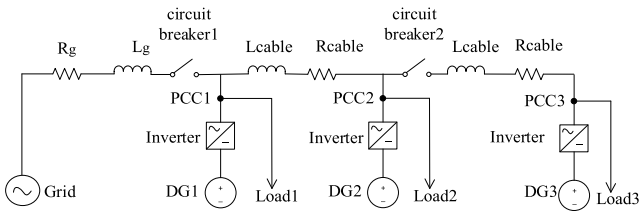

FIGURE 11. Multiple DGs connection mode.

be able to show its ability for islanding detection for multiple DGs connection with negligible effect on the power quality. Figure 11 shows multiple DGs connected to the grid with their respective local loads. As it shows, when circuit breaker 1 is closed and circuit breaker 2 is open, DG1 and DG2 with their relative local loads are connected to the grid. When both circuit breaker 1 and circuit breaker 2 are closed three DGs and their loads are connected to the grid with an underground cable. Each DG operates at a unity power factor with rated active power equal to 100 kW. The values of load parameters are set based on loading quality factor equal to 2.5 with operation at 50 Hz, and underground cable parameters are set based on 200 m length. The loads and cable parameters are illustrated in Table 9 and Table 10 respectively.

TABLE 9. Load parameters for multiple DGs connection mode.

f_{PCC} (Hz)	R_{Load1} (Ω)	R_{Load2} (Ω)	R_{Load3} (Ω)	$L_{Load1,2,3}$ (mH)	$C_{Load1,2,3}$ (μF)
50	1.778	1.455	1.6	2.0372	4973.6

TABLE 10. Underground cable parameters.

Length (m)	R_{cable} (Ω)	L_{cable} (mH)
200	0.0248	0.119

TABLE 11. Detection time for multiple DGs connection mode.

Multiple DGs connection	Detection time (ms)
	Proposed method
Two DGs	180
Three DGs	191

Figure 12 (a) illustrates the PCC frequencies at PCC1 and PCC2 for two DGs connection. Figure 12 (a) confirms the islanding is properly detectable for both DGs. Also, Figure 12 (b) presents PCC frequencies at PCC1, PCC2, and PCC3 for three DGs connection. Figure 12 shows that the proposed islanding method is able to detect islanding in each of the abovementioned conditions at the same time with a negligible difference regardless of the cable connection between DGs. This means that there is synchronization in islanding detection between multiple DGs connection. It is worth noting that multiple DGs connection is tested for the most difficult case, when the resonant frequency is the same as the grid frequency for all loads with zero power mismatch. In case of presence a power mismatch between the load and DG, the detection time is shorter than the tested conditions in this study. Therefore, the proposed islanding detection method is able to detect islanding effectively and rapidly for multiple DGs which are located in a distance from each other in a microgrid with a negligible impact on power quality during grid connection. The detection time for two and three DGs is tabulated in Table 11.

V. EXPERIMENTAL RESULTS

A. PROPOSED ISLANDING DETECTION METHOD PERFORMANCE WITH DIFFERENT Q_f

In this subsection, the proposed islanding detection method is tested under different loading quality factors. The experimental setup parameters are listed in Table 12. Figure 13 shows the experimental setup of the circuit. As shown in Table 12, the inductive and capacitive reactance of the load have been set in such that the reactive power of the load is equal zero. Also, the DG operation has been considered with unity power factor, thus the reactive power mismatch between the load and DG is zero ($\Delta Q = 0$). Also, the load resistance is set so as the load active power is equal to DG rated active power, therefore active power mismatch is zero as well ($\Delta P = 0$).

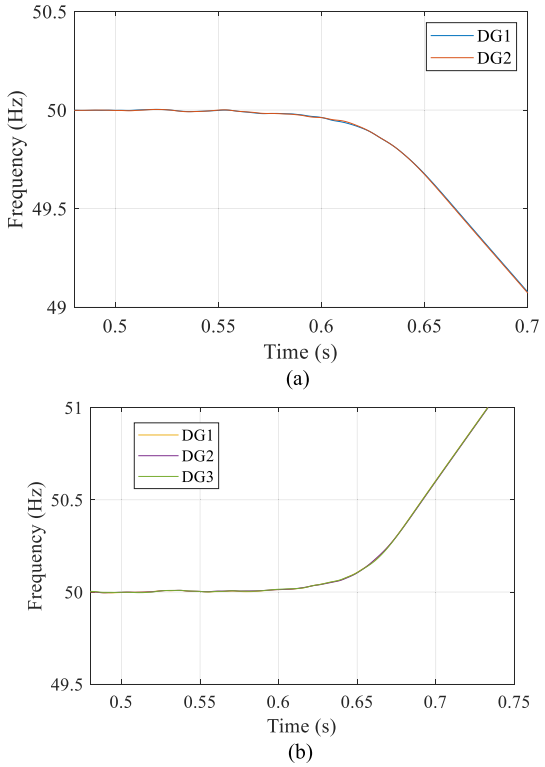

FIGURE 12. Frequency response for multiple DGs connection. (a) two DGs, (b) three DGs.

TABLE 12. Experimental setup parameters.

Grid Parameters	
Frequency	50 Hz
Voltage (line-to-line)	138 V
Load Parameters	
Inductance	71.7 mH
Capacitance	141 µF
Resistance	22.5 Ω
Loading quality factor	1, 1.5, 2, 2,5, 3, 3.5
DG Inverter Parameters	
DG rated active power	845 W
Capacitance-filter	20 µF (Y-connected)
Inductance-filter	2.3 mH
DC voltage	150 V
Switching frequency	5 kHz

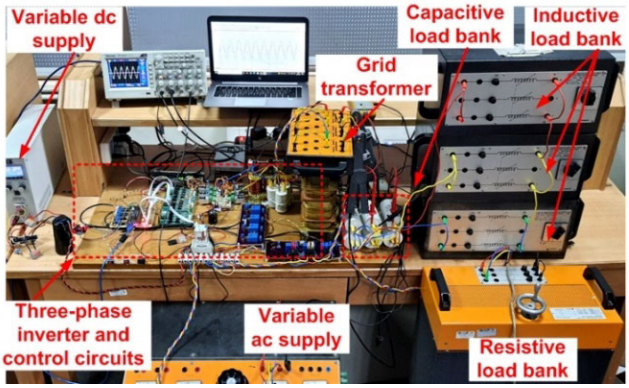

FIGURE 13. Experimental setup for islanding condition.

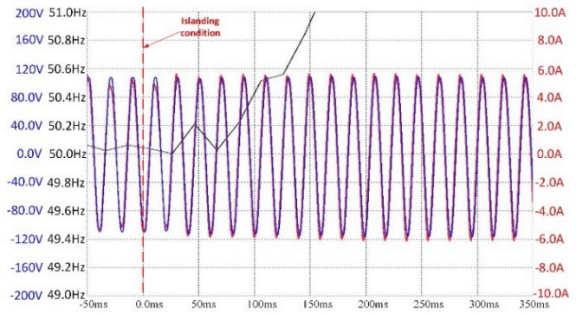

FIGURE 14. Key-wave forms performance of the prospered islanding detection method at $Q_f = 1$.

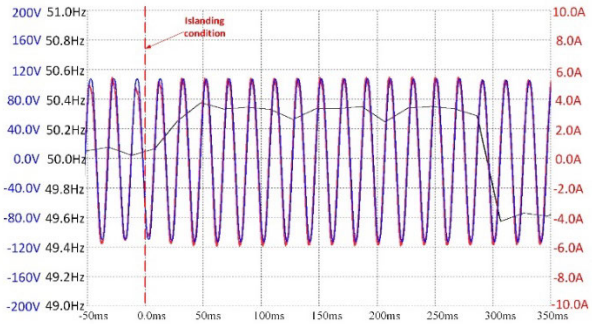

FIGURE 15. Key-wave forms performance of the conventional islanding detection method in [19] at $Q_f = 1$.

These conditions are considered for different loading quality factors as the most difficult cases.

Figure 14 shows the performance of the experimental circuit, when the loading quality factor is set at 1. In this case, active and reactive power mismatch between the load and DG are zero, also the resonant frequency is 50 Hz at the instant of the grid disconnection. As illustrated in Figure 14, the proposed islanding detection method is able to detect the islanding in105 ms for the most difficult case. However, the presented method in [19] fails to detect the islanding as shown in Figure 15. Figure 16 depicts the frequency response of the proposed islanding detection method at different loading quality factors. As it shows the proposed islanding detection method succeeds to detect the islanding under different loading quality factors. The detection time for different loading quality factors is given in Table 13.

B. PROPOSED ISLANDING DETECTION METHOD PERFORMANCE WITH MOTOR LOAD

In this subsection, the performance of the proposed islanding detection method is experimentally evaluated with an induction motor load, which is parallel with a resistance load. The experimental setup is illustrated in Figure 17. Also, the load parameters are shown in Table 14. During this test, the input power of the induction motor has been set at 345 W. The power of the load resistance is adjusted at 450 W during

TABLE 13. Experimental detection time for different Q_f.

Loading quality factor	Detection Time (ms)
1	105
1.5	120
2	122
2.5	140
3	160
3.5	175

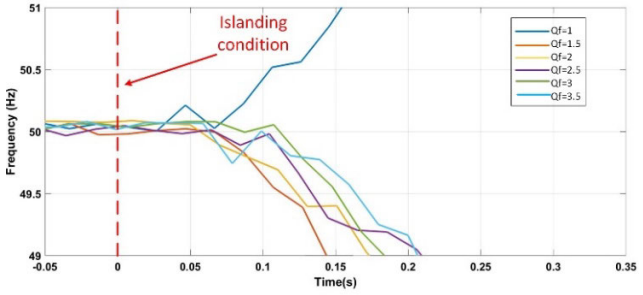

FIGURE 16. Key frequency response of the proposed method for different loading quality factors.

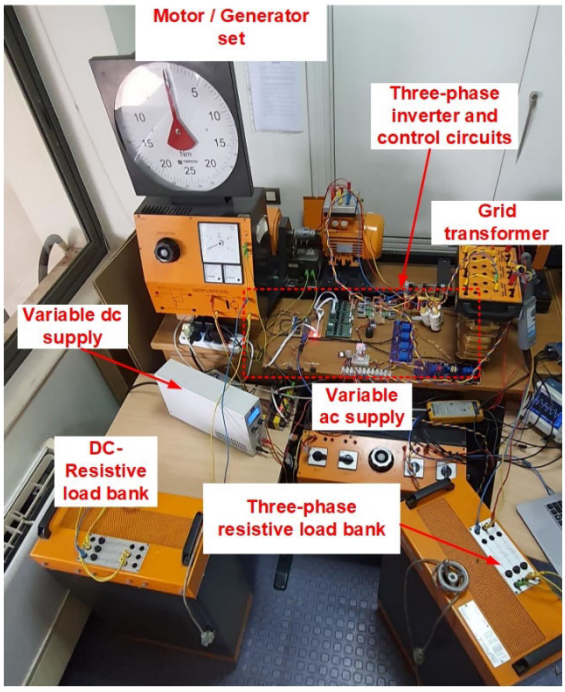

FIGURE 17. Experimental setup for islanding condition with motor load.

case 1, and 530 W during case 2. Also, the DG active power is set at 845 W.

Figure 18 shows the frequency response, when the total load powers including induction motor and the resistance load in case 1 are less than the DG active power. In that case, the PCC frequency rises after the grid disconnection. Therefore, the proposed islanding detection method accelerates the PCC frequency to move up beyond the upper

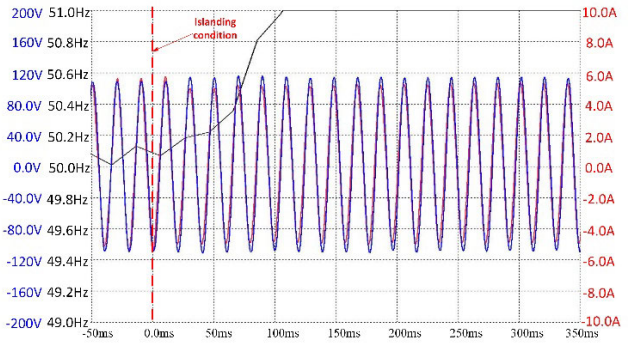

FIGURE 18. Key-wave forms performance of the prospered islanding detection method under motor load and resistance load in case 1.

TABLE 14. Load parameters.

Induction motor parameter	
Voltage (line-to-line)	380 –Y connected
Input power	345 W
Speed	1420 rpm
Resistance load	
Case1	450 W
Case2	530 W

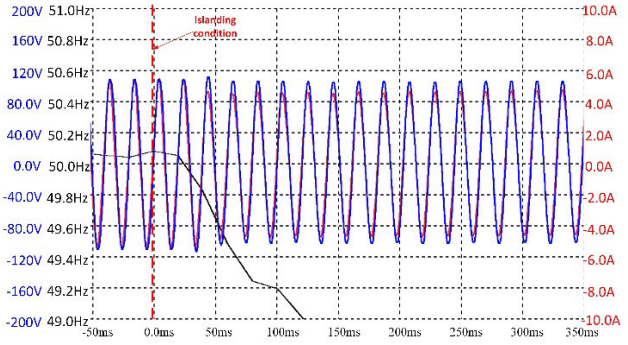

FIGURE 19. Key-wave forms performance of the prospered islanding detection method under motor load and resistance load in case 2.

UOF threshold until islanding is detected within 70 ms. Figure 19 shows the frequency response, when the total load powers including induction motor and the resistance load in case 2 are more than the DG active power. It means that the PCC frequency drops after the grid disconnection. As a result, the proposed islanding detection method forces the PCC frequency to move down beyond the lower UOF threshold for islanding detection in a very short time, which is 60 ms.

VI. CONCLUSION

A modified Q-f droop curve method for islanding detection has been proposed in this paper. The proposed method has been designed such that the inverter-based DG maintains its stable operation during grid-connected, whereas it is unstable when islanding occurs. The design of the proposed method is based on the grid frequency, UOF thresholds, loading quality factor, and rated active power of DG, which are

easily available. Thus, the proposed method enables to be implemented for any DG and grid frequency values without a need for trial and error to choose the system parameters. A UOF relay is sufficient to detect efficiently and rapidly islanding using the proposed method, which reduces the complexity of the detection method. The proposed method has zero NDZ for a wide range of loading quality factors and zero power mismatch between the load and DG. In addition, it has the capability of maintaining stable operation under unbalanced load and load switching conditions. There is no degradation with multiple DGs equipped to the proposed method on the islanding.

REFERENCES

[1] M. Ropp and A. Ellis, "Suggested guidelines for anti-islanding screening," Sandia Nat. Laboratories, New Mexico, CA, USA, Tech. Rep. Sandia Rep. SAND2012-1365, Feb. 2012.

[2] L. E. Miller, J. Schoene, R. Kunte, and G. Y. Morris, "Smart grid opportunities in islanding detection," in *Proc. IEEE Power Energy Soc. Gen. Meeting*, Jul. 2013, pp. 1–4.

[3] C. R. Reddy, B. S. Goud, B. N. Reddy, M. Pratyusha, C. V. V. Kumar, and R. Rekha, "Review of islanding detection parameters in smart grids," in *Proc. 8th Int. Conf. Smart Grid (icSmartGrid)*, Jun. 2020, pp. 78–89.

[4] A. M. Nayak, M. Mishra, and B. B. Pati, "A hybrid islanding detection method considering voltage unbalance factor," in *Proc. IEEE Int. Symp. Sustain. Energy, Signal Process. Cyber Secur. (iSSSC)*, Dec. 2020, pp. 1–5.

[5] S. K. G. Manikonda and D. N. Gaonkar, "Comprehensive review of IDMs in DG systems," *IET Smart Grid*, vol. 2, no. 1, pp. 11–24, Mar. 2019.

[6] C. Li, C. Cao, Y. Cao, Y. Kuang, L. Zeng, and B. Fang, "A review of islanding detection methods for microgrid," *Renew. Sustain. Energy Rev.*, vol. 35, pp. 211–220, Jul. 2014.

[7] F. Mango, M. Liserre, A. Dell'Aquila, and A. Pigazo, "Overview of anti-islanding algorithms for PV systems—Part I: Passive methods," in *Proc. 12th Int. Power Electron. Motion Control Conf.*, Aug. 2006, pp. 1878–1883.

[8] S.-I. Jang and K.-H. Kim, "An islanding detection method for distributed generations using voltage unbalance and total harmonic distortion of current," *IEEE Trans. Power Del.*, vol. 19, no. 2, pp. 745–752, Apr. 2004.

[9] P. K. Ganivada and P. Jena, "Passive islanding detection techniques using synchrophasors for inverter based distributed generators," in *Proc. IEEE PES GTD Grand Int. Conf. Expo. Asia (GTD Asia)*, Mar. 2019, pp. 747–751.

[10] Y. M. Makwana and B. R. Bhalja, "Experimental performance of an islanding detection scheme based on modal components," *IEEE Trans. Smart Grid*, vol. 10, no. 1, pp. 1025–1035, Jan. 2019.

[11] S. Raza, H. Mokhlis, H. Arof, J. A. Laghari, and L. Wang, "Application of signal processing techniques for islanding detection of distributed generation in distribution network: A review," *Energy Convers. Manage.*, vol. 96, pp. 613–624, May 2015.

[12] N. Ahmed and M. Z. R. Khan, "Logistic regression based islanding detection for grid-connected inverter," in *Proc. IEEE Kansas Power Energy Conf. (KPEC)*, Apr. 2021, pp. 1–4.

[13] D. YanLing, D. Ran, W. DongSheng, W. RuoYang, Y. ShaoJun, and N. Hui, "Research on islanding detection method of distributed photovoltaic power supply based on improved AdaBoost algorithm," in *Proc. IEEE Power Energy Soc. Gen. Meeting (PESGM)*, Aug. 2020, pp. 1–5.

[14] A. Yafaoui, B. Wu, and S. Kouro, "Improved active frequency drift anti-islanding detection method for grid connected photovoltaic systems," *IEEE Trans. Power Electron.*, vol. 27, no. 5, pp. 2367–2375, May 2012.

[15] H. Vahedi and M. Karrari, "Adaptive fuzzy Sandia frequency-shift method for islanding protection of inverter-based distributed generation," *IEEE Trans. Power Del.*, vol. 28, no. 1, pp. 84–92, Jan. 2013.

[16] D.-U. Kim and S. Kim, "Anti-islanding detection method using phase-shifted feed-forward voltage in grid-connected inverter," *IEEE Access*, vol. 7, pp. 147179–147190, 2019.

[17] K. Naraghipour, K. Ahmed, and C. Booth, "A comprehensive review of islanding detection methods for distribution systems," in *Proc. 9th Int. Conf. Renew. Energy Res. Appl. (ICRERA)*, Sep. 2020, pp. 428–433.

[18] H. Sun, Y. Zhao, C. Ma, S. Chen, and B. He, "Research on detection technology of islanding effect in the photovoltaic grid-connected power generation system," in *Proc. IEEE Asia–Pacific Conf. Image Process., Electron. Comput. (IPEC)*, Apr. 2021, pp. 252–257.

[19] H. H. Zeineldin, "A *Q–f* droop curve for facilitating islanding detection of inverter-based distributed generation," *IEEE Trans. Power Electron.*, vol. 24, no. 3, pp. 665–673, Mar. 2009.

[20] J. Zhang, D. Xu, G. Shen, Y. Zhu, N. He, and J. Ma, "An improved islanding detection method for a grid-connected inverter with intermittent bilateral reactive power variation," *IEEE Trans. Power Electron.*, vol. 28, no. 1, pp. 268–278, Jan. 2013.

[21] Y. Zhu, D. Xu, N. He, J. Ma, J. Zhang, Y. Zhang, G. Shen, and C. Hu, "A novel RPV (reactive-power-variation) antiislanding method based on adapted reactive power perturbation," *IEEE Trans. Power Electron.*, vol. 28, no. 11, pp. 4998–5012, Nov. 2013.

[22] X. Chen and Y. Li, "An islanding detection method for inverter-based distributed generators based on the reactive power disturbance," *IEEE Trans. Power Electron.*, vol. 31, no. 5, pp. 3559–3574, May 2016.

[23] F. Lin, Y. Huang, K. Tan, J. Chiu, and Y. Chang, "Active islanding detection method using d-axis disturbance signal injection with intelligent control," *IET Gener., Transmiss. Distrib.*, vol. 7, no. 5, pp. 537–550, May 2013.

[24] P. Gupta, R. S. Bhatia, and D. K. Jain, "Average absolute frequency deviation value based active islanding detection technique," *IEEE Trans. Smart Grid*, vol. 6, no. 1, pp. 26–35, Jan. 2015.

[25] X. Chen and Y. Li, "An islanding detection algorithm for inverter-based distributed generation based on reactive power control," *IEEE Trans. Power Electron.*, vol. 29, no. 9, pp. 4672–4683, Sep. 2014.

[26] X. Chen, Y. Li, and P. Crossley, "A novel hybrid islanding detection method for grid-connected microgrids with multiple inverter-based distributed generators based on adaptive reactive power disturbance and passive criteria," *IEEE Trans. Power Electron.*, vol. 34, no. 9, pp. 9342–9356, Sep. 2019.

[27] M. Liu, W. Zhao, Q. Wang, S. Huang, and K. Shi, "A solution to the parameter selection and current static error issues with frequency shift islanding detection methods," *IEEE Trans. Ind. Electron.*, vol. 68, no. 2, pp. 1401–1411, Feb. 2021.

[28] G. Wang and S. University, "Design consideration and performance analysis of a hybrid islanding detection method combining voltage unbalance/total harmonic distortion and bilateral reactive power variation," *CPSS Trans. Power Electron. Appl.*, vol. 5, no. 1, pp. 86–100, Mar. 2020.

[29] A. Yazdani and R. Iravani, "Grid-imposed frequency VSC system," in *Voltage-Sourced Converters in Power Systems: Modelling, Control, and Applications*. Hoboken, NJ, USA: Wiley, Mar. 2010, pp. 204–245.

[30] Z. Ye, A. Kolwalkar, Y. Zhang, P. Du, and R. Walling, "Evaluation of anti-islanding schemes based on nondetection zone concept," *IEEE Trans. Power Electron.*, vol. 19, no. 5, pp. 1171–1176, Sep. 2004.

[31] R. Teodorescu, M. Liserre, and P. Rodriguez, "Islanding detection," in *Grid Converters for Photovoltaic and Wind Power Systems*, 1st ed. Hoboken, NJ, USA: Wiley, Jul. 2011, pp. 93–123.

[32] Z. Ye, R. Walling, L. Garces, R. Zhou, L. Li, and T. Wang, *Study and Development of Anti-Islanding Control for Grid-Connected Inverters*. New York, NY, USA: National Renewable Energy Laboratory, NREL Report, May 2004.

[33] *IEEE Criteria for Utility Interface of Photovoltaic (PV) Systems*, Standard 929-2000, 2000.

KIANOUSH NARAGHIPOUR received the B.Sc. degree from the Amirkabir University of Technology, Iran, and the M.Sc. degree in power distribution engineering from the University of Newcastle upon Tyne, U.K., in 2009. He is currently pursuing the Ph.D. degree with the University of Strathclyde, U.K., as part of the Future Power Networks and Smart Grids CDT. His research interests include power system protection and distribution networks.

IBRAHIM ABDELSALAM (Senior Member, IEEE) received the B.Sc. degree (Hons.) in electrical engineering from the Arab Academy for Science, Technology and Maritime Transport (AASTMT), Cairo, Egypt, Alexandria Campus, in 2006, the M.Sc. degree (Hons.) in electrical engineering from AASTMT, Cairo Campus, in 2009, and the Ph.D. degree in power electronics from the University of Strathclyde, Glasgow, U.K., in 2016. He is currently an Associate Professor with the Electrical Engineering Department, AASTMT. His research interests include power electronic converters and their applications in wind energy conversion systems and advanced control strategies of the multilevel voltage and current source converters.

KHALED H. AHMED (Senior Member, IEEE) received the B.Sc. (Hons.) and M.Sc. degrees from Alexandria University, Egypt, in 2002 and 2004, respectively, and the Ph.D. degree in power electronics applications from the University of Strathclyde, U.K., in 2008. He was appointed as a Professor at Alexandria University, in 2019. He is currently a Reader in power electronics with the University of Strathclyde. He has published more than 140 technical articles in refereed journals and conferences as well as a published textbook titled *High Voltage Direct Current Transmission: Converters, Systems and DC Grids*, a book chapter contribution, and holds a PCT patent PCT/GB2017/051364. His research interests include renewable energy integration, high power converters, offshore wind energy, dc/dc converters, HVDC, and smart grids. He is a Senior Member of the IEEE Power Electronics Society and the IEEE Industrial Electronics Society.

CAMPBELL D. BOOTH (Senior Member, IEEE) received the B.Eng. and Ph.D. degrees in electrical and electronic engineering from the University of Strathclyde, Glasgow, U.K., in 1991 and 1996, respectively. He is currently a Professor and the Head of the Department of Electronic and Electrical Engineering, University of Strathclyde. His research interests include power system protection, plant condition monitoring and intelligent asset management, applications of intelligent system techniques to power system monitoring, protection, and control, knowledge management, and decision support systems.